International Journal of Pharmaceutics 625 (2022) 122096

Contents lists available at ScienceDirect

International Journal of Pharmaceutics

journal homepage: www.elsevier.com/locate/ijpharm

Phosphate decorated lipid-based nanocarriers providing a prolonged mucosal residence time

Nuri Ari Efiana [a,b], Andrea Fürst [a], Ahmad Saleh [a,c], Iram Shahzadi [a], Andreas Bernkop-Schnürch [a,*]

[a] Center for Chemistry and Biomedicine, Department of Pharmaceutical Technology, Institute of Pharmacy, University of Innsbruck, Innrain 80/82, 6020 Innsbruck, Austria
[b] Department of Pharmaceutical Technology, Faculty of Pharmacy, Universitas Ahmad Dahlan, Jl. Prof. Dr. Soepomo, S.H., Janturan, Warungboto, Umbulharjo, Yogyakarta 55164, Indonesia
[c] Department of Pharmacy, Universitas Mandala Waluya, Jl. Jend. A.H. Nasution, Kendari 93231, Southeast Sulawesi, Indonesia

ARTICLE INFO

Keywords:
Lipid-based nanocarriers
Self-emulsifying drug delivery systems (SEDDS)
Solid lipid nanoparticles (SLN)
Nanostructured lipid carriers (NLC)
Charge conversion
Mucosal residence time

ABSTRACT

The aim of this study was to develop phosphate decorated lipid-based nanocarriers including self-emulsifying drug delivery systems (SEDDS), solid lipid nanoparticles (SLN) and nanostructured lipid carriers (NLC) to extend their mucosal residence time. All nanocarriers contained tetradecyltrimethylammonium bromide (TTAB) and polyoxyethylene (9) nonylphenol monophosphate ester (PNPP) for surface decoration. Zeta potential, cytotoxicity, charge conversion and phosphate release studies using isolated intestinal alkaline phosphatase (IAP) and Caco-2 cells were performed. Moreover, the residence time of nanocarriers was determined on porcine intestinal mucosa. Results showed a shift from negative to positive zeta potential due to the addition of TTAB and charge conversion back to a negative zeta potential when also PNPP was added. Up to a concentration of 0.3 %, lipid-based nanocarriers were not toxic. Charge conversion studies with IAP revealed the highest zeta potential shift for $NLC_{TTAB\text{-}PNPP}$ with almost Δ22 mV. Phosphate release studies using isolated IAP as well as Caco-2 cells showed a fast phosphate release for $SEDDS_{TTAB\text{-}PNPP}$, $SLN_{TTAB\text{-}PNPP}$ and $NLC_{TTAB\text{-}PNPP}$. $SLN_{TTAB\text{-}PNPP}$ and $NLC_{TTAB\text{-}PNPP}$ provided the highest increase in mucosal residence time that was 4-fold more prolonged than that of blank formulations. In conclusion, phosphate modified lipid-based nanocarriers can essentially prolong the intestinal residence time of their payload.

1. Introduction

The treatment efficacy of many drugs is limited by a too short residence time on mucosal membranes. As in case of local treatments drugs are eliminated too rapidly from the mucosal target tissues, just a temporarily and often insufficient therapeutic effect can be achieved (Kali et al., 2022). In case of systemic drug delivery via mucosal membranes, uptake into the systemic circulation is in particular for poorly absorbed drugs too low when the time for the absorption process is short. The design of drug delivery systems providing a prolonged residence time on mucosal membranes is therefore highly on demand. As the mucus gel layer covering mucosal membranes has a negative charge because of sialic and sulphonic substructures, cationic polymers and nanoparticles are immobilized in mucus via ionic interactions (Griffin et al., 2016). As these interactions are already taking place on the loose outer mucus layer that is rapidly eliminated from the mucosal surface, however, a prolonged mucosal residence time cannot be achieved with such cationic drug carrier systems (O'Driscoll et al., 2019).

A promising strategy in order to address this dilemma are charge converting drug delivery systems. Nanocarriers exhibiting an anionic surface charge were already shown to diffuse into the firm deeper mucus reaching even the underlying epithelium, where they convert their surface charge to positive due to the cleavage of phosphate substructures on their surface by the membrane bound enzyme alkaline phosphatase (Le-Vinh et al., 2022). So far, however, the potential of such charge converting nanocarriers to provide a prolonged mucosal residence time has not been evaluated.

It was therefore the aim of this study to design phosphate decorated lipid-based nanocarriers providing a prolonged mucosal residence time via the formation of ionic bonds between the nanocarriers and the

* Corresponding author.
E-mail address: andreas.bernkop@uibk.ac.at (A. Bernkop-Schnürch).

https://doi.org/10.1016/j.ijpharm.2022.122096
Received 5 July 2022; Received in revised form 3 August 2022; Accepted 5 August 2022
Available online 10 August 2022

Table 1
Composition of SEDDS formulations. O1, O2, S1 and S2 refer to glyceryl tricaprylate, caprylic/capric triglyceride, polyoxyl 35 castor oil and polyoxyl 40 hydrogenated castor oil, respectively.

Code	Solvents (oils)(mg)		Surfactants (mg)		Co-solvent (mg)	Surface Modifiers (mg)		Marker (mg)
	O1	O2	S1	S2	Propylene Glycol	TTAB	PNPP	FDL
$SEDDS1_{blank}$	300	–	400	–	300	–	–	2.5
$SEDDS2_{blank}$	–	300	–	400	300	–	–	2.5
$SEDDS1_{TTAB}$	300	–	400	–	300	5	–	2.5
$SEDDS2_{TTAB}$	–	300	–	400	300	5	–	2.5
$SEDDS1_{TTAB+PNPP}$	300	–	400	–	300	5	30	2.5
$SEDDS1_{TTAB+PNPP}$	–	300	–	400	300	5	30	2.5

mucosa due to charge conversion from negative to positive. Lipid nanocarriers including self-emulsifying drug delivery systems (SEDDS), solid lipid nanoparticles (SLN) and nanostructured lipid carriers (NLC) were selected as carriers in this study. As lipid nanocarriers, they provide biocompatible and non-toxic properties as well as can increase the effectiveness of drugs therapy. In addition, NLC provide high drug loading since they consist of solid and liquid lipids as carrier matrix (Severino et al., 2012; Wissing et al., 2004). Lipid-based nanocarriers were decorated with tetradecyltrimethylammonium bromide (TTAB) as a cationic surfactant supplying a positive charge and polyoxyethylene (9) nonylphenol monophosphate ester (PNPP) as phosphorylated surfactant providing a net negative charge. Zeta potential and particle size of lipid-based formulations before and after the modification were determined. Furthermore, cytotoxicity of these formulations was evaluated on Caco-cells via resazurin assay. Charge conversion and phosphate release studies utilizing isolated intestinal alkaline phosphatase (IAP) as well as Caco-2 cells were performed. Moreover, the residence time of these lipid nanocarriers was determined on porcine intestinal mucosa.

2. Materials and methods

2.1. Materials

Captex 8000 (glyceryl tricaprylate) and Captex 300 EP (caprylic/capric triglycerride) were supplied by Abitec, USA. Dynasan 116 (glycerol tripalmitate) was obtained from IOI Oleo GmbH, Germany. Transcutol HP (diethylene glycol monoethyl ether) was received from Gattefosse, France. Cremophor EL (polyoxyl 35 castor oil), Kolliphor RH 40 (polyoxyl 40 hydrogenated castor oil), propylene glycol, oleic acid, Brij 93 (polyethylene glycol oleyl ether), trimethyl tetradecyl ammonium bromide (TTAB), fluorescein dilaurate (FDL), bovine intestinal alkaline phosphatase (IAP, ≥10 DEA units/mg protein) and phosphatase inhibitor cocktail 2 (PIC2) were provided by Sigma-Aldrich, Germany. Polyoxyethylene (9) nonylphenol monophosphate ester (PNPP) was obtained from Ashland Inc, Switzerland. Porcine intestine was supplied by slaughterhouse, Innsbruck, Austria.

2.2. Methods

2.2.1. Preparation of lipid nanocarrier formulations

2.2.1.1. Preparation of self-emulsifying drug delivery systems (SEDDS). SEDDS formulations were prepared by mixing all components including oil, surfactant and cosolvent as shown in Table 1 using a vortex mixer for 20 min, followed by shaking in a thermomixer (Eppendorf, Germany) at 1000 rpm at a temperature of 60ºC for about one hour. For the purpose of mucosa residence time studies, 0.25 % (m/v) FDL as a marker was incorporated in the lipid nanocarriers by mixing in a thermomixer at 60ºC and a speed of 1000 rpm for 20 min. Modified SEDDS formulations were prepared by addition of TTAB and PNPP according to Table 1.

2.2.1.2. Preparation of solid lipid nanoparticles (SLN) and nanostructured lipid carriers (NLC). Preparation of SLN and NLC was carried out based on modifications of previously published methods (Luan et al., 2014; Schubert and Müller-Goymann, 2003). Briefly, the lipid phase was prepared by melting the lipid components as shown in Table 2 with ethanol at 68 °C using a thermomixer at 1000 rpm for 30 min. Glycerol tripalmitate was used as a solid lipid component in the lipid phase of SLN and NLC formulations, whereas in the NLC formulation, oleic acid was added as a liquid lipid. FDL serving as marker was incorporated by dissolving it in 50 μL of ethanol prior to be added to the lipid phase. Mixing was continued for 20 min to evaporate ethanol. The aqueous phase containing the hydrophilic surfactant at the same temperature was added dropwise to the lipid phase while stirring continuously using a thermomixer at a temperature of 68 °C and a speed of 650 rpm for 20

Table 2
Composition of SLN and NLC formulations prepared in 1 mL of demineralized water. L1, L2, S1, S2, S3 and CS refer to glycerol tripalmitate, oleic acid, polyoxyl 35 castor oil, polyoxyl 40 hydrogenated castor oil, polyethylene glycol oleyl ether and diethylene glycol monoethyl ether, respectively.

Code	Solid lipid (mg)	Liquid lipid (mg)	Surfactants (mg)			Co-surfactant (mg)	Surface modifiers (mg)		Marker (mg)
	L1	L2	S1	S2	S3	CS	TTAB	PNPP	FDL
$SLN1_{blank}$	18	–	12	–	6	–	–	–	2.5
$SLN2_{blank}$	18	–	–	12	6	–	–	–	2.5
$NLC1_{blank}$	12	6	12	–	–	6	–	–	2.5
$NLC2_{blank}$	12	6	–	12	–	6	–	–	2.5
$SLN1_{TTAB}$	18	–	12	–	6	–	8	–	2.5
$SLN2_{TTAB}$	18	–	–	12	6	–	8	–	2.5
$NLC1_{TTAB}$	12	6	12	–	–	6	8	–	2.5
$NLC2_{TTAB}$	12	6	–	12	–	6	8	–	2.5
$SLN1_{TTAB+PNPP}$	18	–	12	–	6	–	8	20	2.5
$SLN2_{TTAB+PNPP}$	18	–	–	12	6	–	8	20	2.5
$NLC1_{TTAB+PNPP}$	12	6	12	–	–	6	8	20	2.5
$NLC2_{TTAB+PNPP}$	12	6	–	12	–	6	8	20	2.5

min. Mixing was continued at room temperature for 30 min prior to centrifugation at 3500 rpm at a temperature of 4 °C for 20 min. The supernatant containing SLN and NLC was collected and used for further experiments.

For the preparation of surface decorated SLN and NLC as listed in Table 2, TTAB and PNPP were added to the lipid phase followed by the addition of the aqueous phase. TTAB was dissolved in 50 μL of ethanol prior to be added to the lipid phase, whereas PNPP was added directly. All further preparation steps were the same as described above.

2.2.2. Characterization of lipid nanocarrier formulations

SEDDS, SLN and NLC were characterized regarding size, polydispersity index, and zeta potential utilizing a Zetasizer (Nano-ZSP, Malvern P analitycal, UK). The buffer used within this experiment was 20 mM HEPES buffer pH 7.0 containing 150 mM NaCl (HBS). This buffer was also used for further studies. For zeta potential measurements, samples were dispersed (1:100) in HBS and further diluted 10 times with water to adjust conductivity during measurement at about ~ 1 mS/cm (Le-Vinh et al., 2021). The buffer capacity of this dilution was 0.79 μmol/mL/ΔpH which is still in the range of the buffer capacity of intestinal fluids(Hens et al., 2017).

2.2.3. Studies of cytotoxicity on Caco-2 cells

Cytotoxicity of formulations was evaluated on Caco-2 cells. For this purpose, Caco-2 cells were grown in 24-well plates in an incubator at 37ºC. The feeding of cells was conducted every-two days with red minimum essential medium (red MEM) containing 10 % fetal bovine serum and 1 % penicillin antibiotic till two weeks of cultivation. Afterwards, cells were washed using sterile HBS (HBSS), and incubated with the HBSS at 37ºC for 30 min, followed by replacing the buffer with 500 μL of 0.1 % dispersion of sample in HBSS prior to be incubated at 37ºC for 4 h. HBSS and Triton-X were used as negative and positive controls, respectively. After completion of incubation, samples were removed and cells were rinsed using HBSS followed by the addition of 250 μL of 2.2 mM resazurin solution and incubation at 37 °C for 3 h. Cell viability was determined by quantifying the fluorescein intensity of each sample using Tecan microplate reader at an excitation wavelength of 540 nm and an emission wavelength of 590 nm.

2.2.4. Charge conversion studies

Concisely, 20 μL of IAP solution were added to 1 mL of 1 % formulation dispersion in HBS, yielding a final enzyme activity of 2 U/mL which does not exceed the enzyme level on human intestinal mucosa (Hirano et al., 1987). Thereafter, the mixture was incubated in a thermomixer at 37 °C and a speed of 500 rpm prior to zeta potential measurements(Akkuş-Dağdeviren et al., 2021; Perera et al., 2015).

2.2.5. Phosphate release studies

2.2.5.1. Malachite green phosphate assay. Released phosphate was quantified utilizing the malachite green (MLG) assay(Baykov et al., 1988; Carter and Karl, 1982). Succinctly, malachite green phosphate reagent was prepared freshly by mixing 200 μL of Tween 20 (11 % m/v in water) with 5 mL solution of malachite green oxalate (0.15 % (m/v) in 3.6 M H_2SO_4) in a thermomixer at a speed of 750 rpm, at room temperature for 20 min. Mixing was continued for 20 min after dropwise addition of 3 mL of 8 % (m/v) ammonium molybdate tetrahydrate solution in water. For the purpose of phosphate quantification, 5 μL of 3.6 M H_2SO_4 was added to 50 μL sample to terminate the enzymatic reaction, followed by the addition of 100 μL of malachite green reagent and mixed for 15 min prior to the phosphate quantification using Tecan (Spark® Multimode Microplate Reader, Switzerland) at a wavelength of 630 nm. A standard curve was created from a series of 9–115 μM KH_2PO_4 solution with the same procedure as for sample preparation.

2.2.5.2. Enzymatic phosphate cleavage assay using isolated IAP. Briefly, samples of SEDDS, SLN and NLC were dispersed in 1 % HBS followed by the addition of 20 μL of IAP prior to the incubation in a thermomixer at 37 °C and a speed of 500 rpm for 4 h. The same procedure but without IAP was also carried out for control. At predetermined time points, aliquots of 50 μL were withdrawn and 5 μL of 3.6 M H_2SO_4 was added to stop the enzymatic reaction. Thereafter, the released phosphate was quantified using the malachite green assay as described above.

2.2.5.3. Enzymatic phosphate cleavage assay on Caco-2 cells. Phosphate cleavage was also analyzed on Caco-2 cells expressing IAP. Cells were grown until a monolayer was formed in approximately 12 to 14 days by feeding every-two days with red minimum essential medium (MEM). Cells were seeded in 24-well plates at a density of 25,000 cells/well in an incubator containing 5 % of CO_2 at 37 °C. On the day of experiment, cells were washed two times with 25 mM HEPES buffer pH 7.4 containing 268 mM glucose followed by incubation for one hour with the same buffer comprising of PIC2 as control or merely buffer. Afterwards, the buffer was exchanged with 500 μL of sample diluted (1:1000) in glucose-HEPES buffer prior to incubation for 4 h. At predetermined time points, aliquots of 50 μL were withdrawn for phosphate quantification utilizing malachite green assay as described above (Akkuş-Dağdeviren et al., 2021).

2.2.6. Residence time studies on porcine intestinal mucosa

The capability of droplets and nanocarriers containing FDL as a marker to adhere on porcine intestinal mucosa was determined using a modified falling liquid film method (Gradauer et al., 2012). Three groups of samples namely blank formulations, TTAB-PNPP modified formulations with intestinal pre-incubation using phosphatase enzyme inhibitor (PIC2) and TTAB-PNPP modified formulations without pre-incubation of intestine using PIC2 were tested.

Briefly, the intestine was cut in a size of 4 cm × 10 cm and attached to a semi-cylindrical plastic tube with a facing up of mucosa followed by placing in a tightly closed humidity-maintained chamber to keep it moist prior to be put in an incubator at 37 ºC with controlled humidity. Subsequently, the intestine was incubated with 1 % (v/v) PIC2 solution in HBS for one hour prior to experiment. In parallel, incubation with HBS omitting PIC2 was also conducted. Thereafter, 500 μL of 1 % dispersion of lipid formulations in HBS was applied to the intestinal mucosa evenly followed by incubation at 37 °C for 4 h. The intestinal mucosa was rinsed using HBS at a rate of 1 mL/min for 5 min prior to be extracted by shaking using 5 mL of 96 % ethanol (v/v) at 37 °C for 30 min. Subsequently, the samples were centrifuged at 12000 rpm at 4ºC for 20 min continued by hydrolyzing FDL due to the addition of 100 μL of 5 M NaOH to 500 μL of samples withdrawn from the supernatant. To quantify the FDL content, the hydrolyzed samples were measured using Tecan microplate reader at an excitation and emission wavelength of 485 nm and 535 nm, respectively.

2.2.7. Statistical data analysis

In order to compare the effect of surface modification using TTAB and PNPP on lipid nanocarriers properties, one-way ANOVA followed by Tukey HSD test was carried out, while the independent sample *t*-test was used to define the impact of surface modification of each composition in lipid nanocarrier formulations on mucosal residence time. The program software namely SPSS 17 was used to perform the statistical analysis.

3. Results and discussion

3.1. Preparation and characterization of lipid nanocarrier formulations

Phosphate decorated lipid-based nanocarriers were developed via incorporation of a phosphorylated surfactant into nanocarriers including SEDDS, SLN and NLC. The properties of lipid nanocarriers

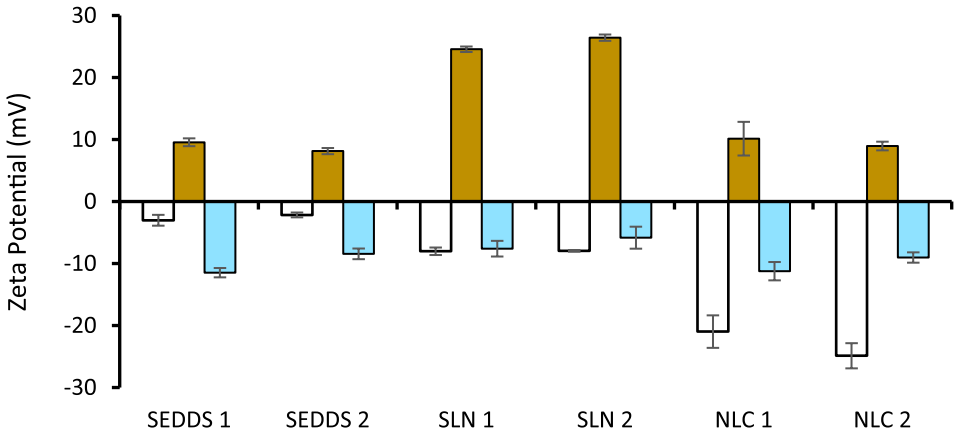

Fig. 1. Zeta potential values of $SEDDS_{blank}$, SLN_{blank} and NLC_{blank} (white bars), $SEDDS_{TTAB}$, SLN_{TTAB} and NLC_{TTAB} (brown bars) and $SEDDS_{TTAB\text{-}PNPP}$, $SLN_{TTAB\text{-}PNPP}$ and $NLC_{TTAB\text{-}PNPP}$ (blue bars). Data are presented as mean ± SD (n = 3).

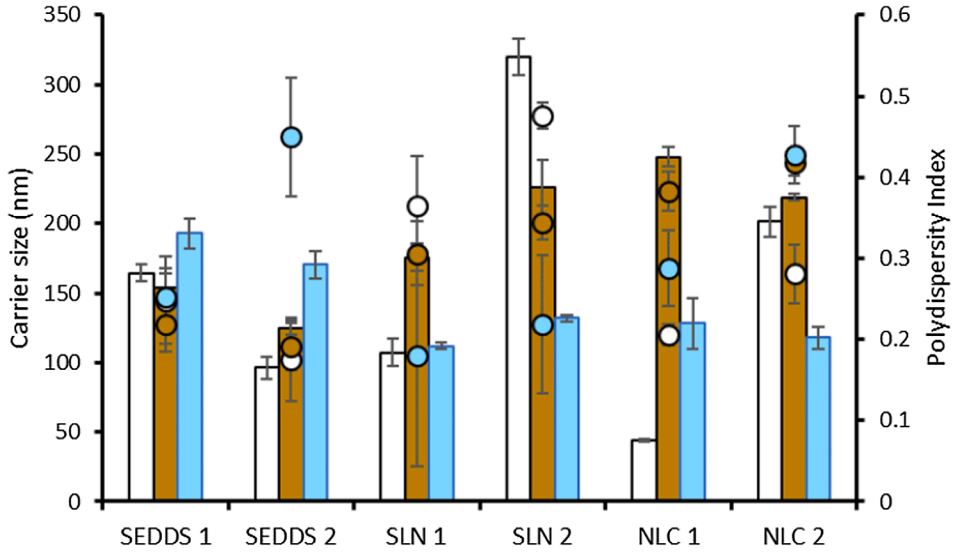

Fig. 2. Mean droplet size (bar) and PDI (dot) values of $SEDDS_{blank}$, SLN_{blank} and NLC_{blank} (white), $SEDDS_{TTAB}$, SLN_{TTAB} and NLC_{TTAB} (brown) and $SEDDS_{TTAB\text{-}PNPP}$, $SLN_{TTAB\text{-}PNPP}$ and $NLC_{TTAB\text{-}PNPP}$ (blue). Data are presented as mean ± SD (n = 3).

before and after modification were characterized. Polyoxyethylene surfactants, namely polyoxyl 35 castor oil and polyoxyl 40 hydrogenated castor oil were used in present study. These surfactants provide the ability to produce PEGylated nanocarriers which can inhibit lipid digestion thereby increasing bioavailability (Feeney et al., 2014). In lipid nanocarriers, the hydrophilic moiety of these surfactants, namely glyceryl polyoxyethylene, is on the surface determining the zeta potential by adsorption of ions. Due to the similarity of the hydrophilic moieties, each pair of unmodified nanocarriers, $SEDDS1_{blank}$ and $SEDDS2_{blank}$, $SLN1_{blank}$ and $SLN2_{blank}$, as well as $NLC1_{blank}$ and $NLC2_{blank}$, exhibited almost the same zeta potential as shown in Fig. 1. The negative charge of these nanocarriers exhibiting a polyoxyethylene surface is in line with previous research on nanomicelles (Grotz et al., 2017; Liu et al., 2016), nanodroplets (Kurpiers et al., 2020; Sharifi et al., 2019; Suchaoin et al., 2016), nanolipids (Almousallam et al., 2015) as well as nanoparticles (Sis and Birinci, 2009) displaying also a polyoxyethylene surface.

Regarding the size of unmodified nanocarriers, the addition of polyoxyl 40 hydrogenated castor oil resulted in larger particles, except SEDDS formulations as shown in Fig. 2. The determined particle size was assumed for single particles or droplets and not aggregates (flocculate) since the negative charge of nanocarriers repulses them from each other. Since surfactants "stand-up" on the surface of nanocarrier, total surface area of surfactant is the product of cross-sectional area and the number of surfactant molecules. Therefore, at the same mass, polyoxyl 40 hydrogenated castor oil exhibiting a higher molecular weight has a lower total surface area than polyoxyl 35 castor oil, since both surfactants have the same cross-sectional area. The ratio of total surface area of surfactant to lipid volume determines subsequently the nanocarrier's size.

Furthermore, the match between the HLB of surfactant and the rHLB of lipid has an impact on the size of lipid nanocarriers (Keck et al., 2014). The difference between surfactant HLB and lipid rHLB in SLN_{blank} and $NLC1_{blank}$ was lower than that in $SLN2_{blank}$ and $NLC2_{blank}$, respectively, resulting in a smaller size of $SLN1_{blank}$ and $NLC1_{blank}$ than of their counterparts. The combination of polyoxyl 35 castor oil and polyethylene glycol oleyl ether in $SLN1_{blank}$ provides a HLB of 10.1 that is closer to the rHLB of glycerol tripalmitate than that of the combination of polyoxyl 40 hydrogenated castor oil and polyethylene glycol oleyl ether. The combination of glycerol tripalmitate and oleic acid in NLC yielded an rHLB of 10.7 that is closer to the HLB of surfactants mixture in $NLC1_{blank}$ than in $NLC2_{blank}$. SEDDS formulations containing polyoxyl 40 hydrogenated castor oil showed a smaller size. It is likely that the conformity between HLB and rHLB in $SEDDS2_{blank}$ is higher than that in $SEDDS1_{blank}$.

Lipid nanocarriers were decorated with TTAB and PNPP to modulate their zeta potential. The concentrations of TTAB and PNPP as indicated

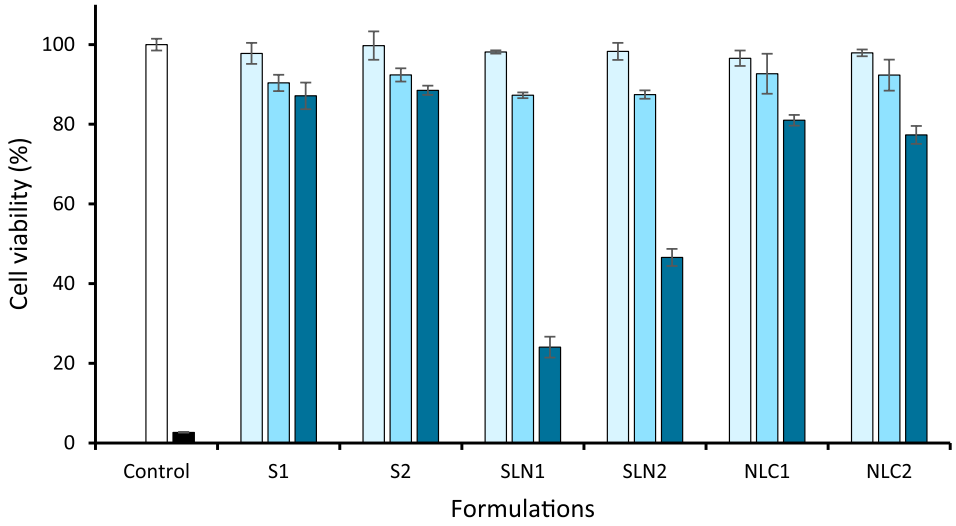

Fig. 3. Cell viability of Caco-2 cells incubated with formulations in 24 well plates for 4 h. White, black, light blue, blue and dark blue bars represent negative control, positive control and 0.1 %, 0.3 % and 0.5 % of formulations containing TTAB-PNPP, respectively. Data are presented as mean ± SD (n = 3).

in Tables 1 and 2 were chosen based on orientating studies of formulations. As TTAB bears a quaternary ammonium substructure, it exhibits a permanent positive charge. In Fig. 1, the ability of this quaternary ammonium ion to increase the zeta potential is depicted. The highest zeta potential shift was observed for $SLN2_{TTAB}$ with almost Δ35 mV. On the one hand, the addition of TTAB increases the ratio of total surface area to lipid volume triggering size reduction. On the other hand, however, the ionic surfactant increases HLB resulting in the decrease in HLB and rHLB conformity. In case of $SEDDS2_{TTAB}$, $SLN1_{TTAB}$ and $NLC1_{TTAB}$, TTAB increased significantly ($p < 0.05$) the particle size by 1.3, 1.6 and 5.7-fold, respectively. Modification of lipid nanocarriers using PNPP provided negative charges originating from the phosphate moiety as shown in Fig. 1. The addition of PNPP increased the total surface area of surfactant mixture resulting in a significant ($p < 0.05$) reduction in the size of nanocarriers compared to TTAB modified formulations as depicted in Fig. 2.

3.2. Cytotoxicity studies on Caco-2 cells

The cytotoxic effect of lipid nanocarriers was evaluated utilizing resazurin assay on Caco-2 cells as shown in Fig. 3. At a concentration of 0.1 %, all lipid nanocarriers including $SEDDS_{TTAB\text{-}PNPP}$, $SLN_{TTAB\text{-}PNPP}$ and $NLC_{TTAB\text{-}PNPP}$ exhibited cell viability ≥ 96 %, whereas at a concentration of 0.3 % it was ≥ 87 %. Increasing the concentration of $SLN1_{TTAB\text{-}PNPP}$ and $SLN2_{TTAB\text{-}PNPP}$ to 0.5 % resulted in a decrease in cell viability to 24 % and 46 %, respectively, whereas all other formulations provided still a viability of more than 77 %. Based on these results, it can be concluded that all formulations up to a concentration of 0.3 % were not toxic as indicated by a cell viability of greater than 85 % (López-García et al., 2014). Since the resting volume of gastric fluid is about 35 ml (Mudie et al., 2014), for the oral administration of one gram of these formulations at least 298 mL of water have to be co-administrated to obtain a final concentration of 0.3 %, that was shown to be non-toxic in our experiments.

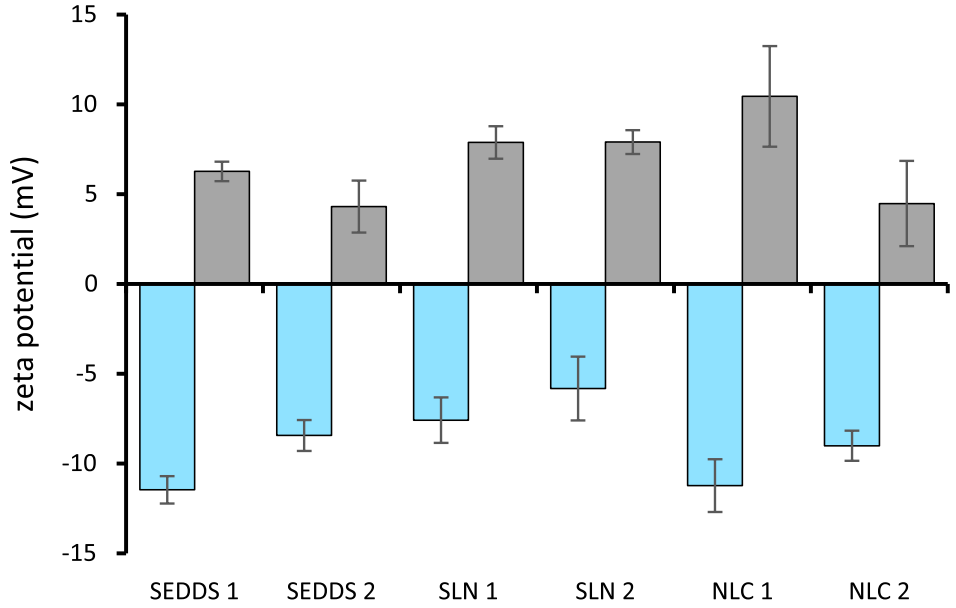

Fig. 4. Zeta potential of $SEDDS_{TTAB\text{-}PNPP}$, $SLN_{TTAB\text{-}PNPP}$ and $NLC_{TTAB\text{-}PNPP}$ formulations before (blue bars) and after (grey bars) incubation with isolated IAP for 4 h. Data are presented as mean ± SD (n = 3).

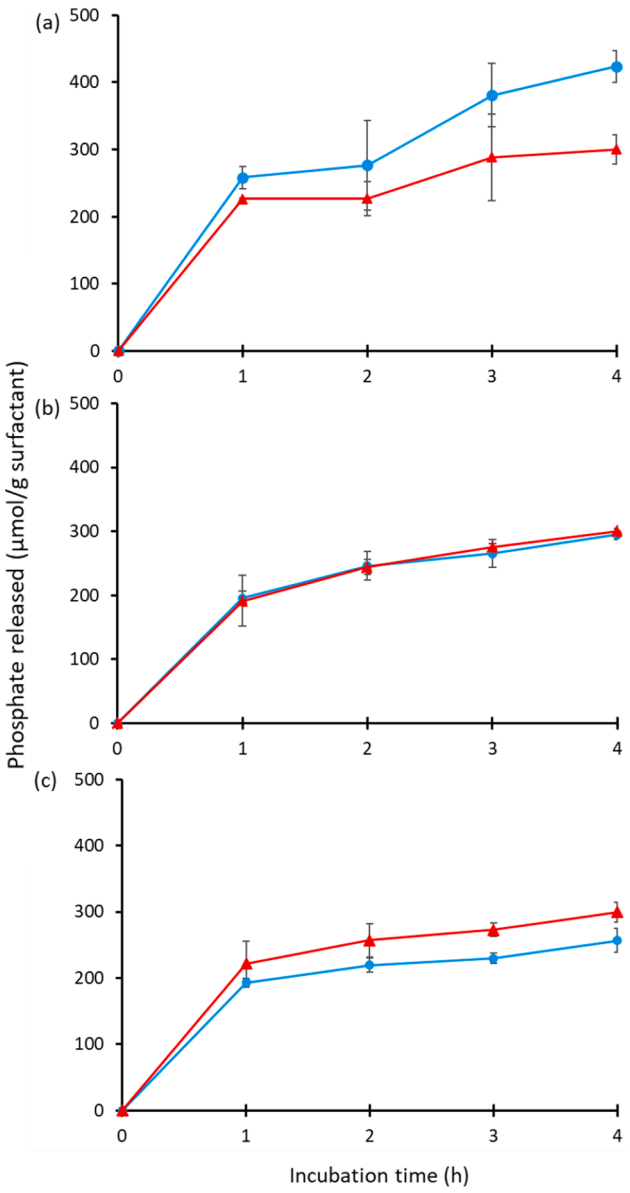

Fig. 5. Phosphate release of 1:100 diluted formulations of (a) $SEDDS_{TTAB\text{-}PNPP}$ (b) $SLN_{TTAB\text{-}PNPP}$ and (c) $NLC_{TTAB\text{-}PNPP}$ by enzymatic cleavage with isolated IAP. Each nanocarrier consists of $SEDDS1_{TTAB\text{-}PNPP}$, $SLN1_{TTAB\text{-}PNPP}$ and $NLC1_{TTAB\text{-}PNPP}$ (—●—) and $SEDDS2_{TTAB\text{-}PNPP}$, $SLN2_{TTAB\text{-}PNPP}$ and $NLC2_{TTAB\text{-}PNPP}$ (—▲—). Data are presented as mean ± SD (n = 3).

3.3. Charge conversion studies

IAP, a member of the alkaline phosphatase family, being expressed on intestinal epithelial cells was used for charge conversion studies. This enzyme is located on the apical surface of intestinal membrane (Ghosh et al., 2021). It has been used for drug delivery in previous studies (Kurpiers et al., 2020; Akkuş-Dağdeviren et al., 2019; Wolf et al., 2020). In this study, the capability of IAP to convert the charge of lipid nanocarriers from negative to positive was evaluated as depicted in Fig. 4. The shift in zeta potential originating from cleavage of phosphate esters by IAP was also investigated in several studies by our research group using various phosphorylated surfactants (Akkuş-Dağdeviren et al., 2021; Wolf et al., 2020; Nazir et al., 2019). As shown in Fig. 4, all formulations exhibited a shift in zeta potential from negative to positive ranging from Δ13 to Δ22 mV. PNPP was used in previous studies as a surface modifier for SEDDS droplets utilizing a PEGylated surfactant at concentrations of 18 % (Kurpiers et al., 2020) and 36.7 % (Akkuş-Dağdeviren et al., 2021) resulting in a shift in zeta potential of Δ33 mV and Δ22 mV, respectively. The higher surfactant concentration used in the SEDDS formulation of the present study led to a lower zeta potential shift. The degree of shift in the zeta potential which was inversely proportional to the polyoxyethylene concentration might describe the effect of PEG corona density on phosphate cleavage (Rabanel et al., 2014).

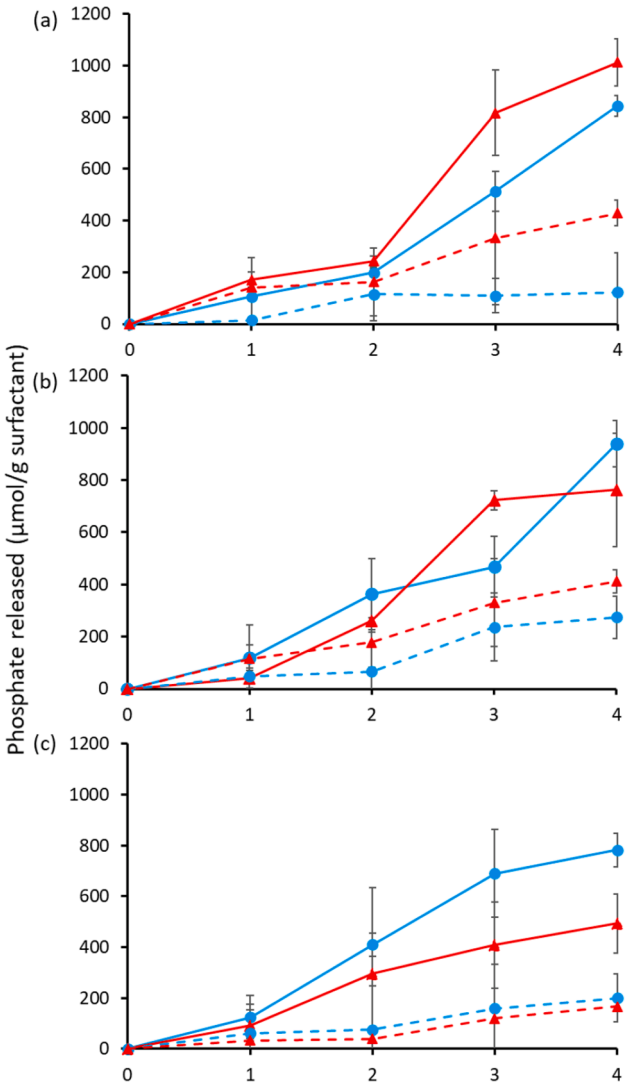

Fig. 6. Phosphate release of 1:100 diluted formulations of (a) $SEDDS_{TTAB\text{-}PNPP}$ (b) $SLN_{TTAB\text{-}PNPP}$ and (c) $NLC_{TTAB\text{-}PNPP}$ by enzymatic cleavage using Caco-2 cells. Each nanocarrier consists of $SEDDS1_{TTAB\text{-}PNPP}$, $SLN1_{TTAB\text{-}PNPP}$ and $NLC1_{TTAB\text{-}PNPP}$ (without inhibitor: —●—, with inhibitor: - -●- -) and $SEDDS2_{TTAB\text{-}PNPP}$, $SLN2_{TTAB\text{-}PNPP}$ and $NLC2_{TTAB\text{-}PNPP}$ (without inhibitor: —▲—, with inhibitor: - -▲- -). Data are presented as mean ± SD (n = 3).

3.4. Phosphate release studies

In Fig. 5, phosphate release starting with a burst release within the first hour of about 250, 190 and 200 µmol/g surfactant per hour for $SEDDS_{TTAB\text{-}PNPP}$, $SLN_{TTAB\text{-}PNPP}$ and $NLC_{TTAB\text{-}PNPP}$ formulations, respectively, is shown. After one hour of incubation, the rate of phosphate release was determined to be 40, 37 and 24 µmol/g surfactant per hour for $SEDDS_{TTAB\text{-}PNPP}$, $SLN_{TTAB\text{-}PNPP}$ and $NLC_{TTAB\text{-}PNPP}$, respectively. The hydrophilic spacer connecting the phosphate group with the lipophilic moiety in PNPP contains 9 oxyethylene subunits, whereas the surfactants containing polyoxyethylene such as polyoxyl 35 castor oil and polyoxyl 40 hydrogenated castor oil exhibit at least 11 oxyethylene

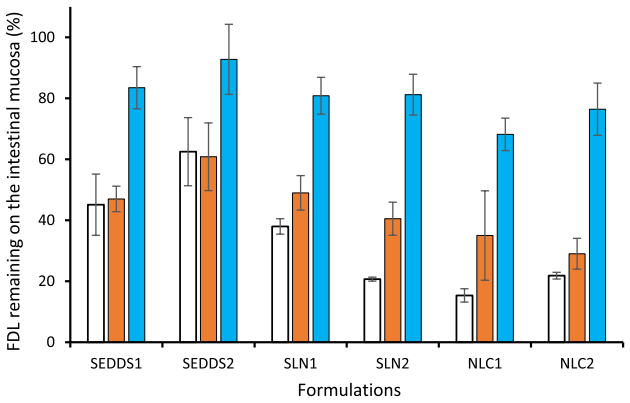

Fig. 7. Percentage of FDL remaining on the intestinal mucosa after 4 h of experiment, in case of control (blank formulations) (white bars), formulations containing TTAB-PNPP in the presence of 1 % (v/v) phosphatase inhibitor cocktail II (PIC2) (orange bars) and formulations containing TTAB-PNPP in the absence of PIC2 (blue bars). Data are presented as mean ± SD (n = 3).

subunits. Due to the small difference in the length of the polyoxyethyl spacer, and the possibility of various conformations of the PEG corona on the nanocarrier surface (Rabanel et al., 2014), it can be assumed that the position of phosphate groups on the corona were responsible for the phosphate release profile. Phosphate groups being covered by the polyoxyethylene corona or glyceryl groups of surfactants were more difficult to be cleaved by IAP, likely resulting in slow phosphate release after one hour of incubation. Phosphate release studies were also performed utilizing IAP-expressing Caco-2 cells. As depicted in Fig. 6, phosphate release was initiated at a slow rate within the first two hours followed by a faster release thereafter. In contrast, experiments using isolated IAP showed a rapid release of phosphate within the first hour. This observation might the time required for the lipid nanocarrier to propagate on Caco-2 cells bearing IAP prior to phosphate release. The order of phosphate release from highest to lowest was $SEDDS_{TTAB\text{-}PNPP}$, $SLN_{TTAB\text{-}PNPP}$ and $NLC_{TTAB\text{-}PNPP}$, which was in line with results of phosphate release studies using isolated IAP.

3.5. Mucosal residence time studies

Results of mucosal residence time studies showed that all phosphate decorated lipid nanocarriers provide significantly ($p < 0.05$) higher FDL concentrations remaining on the mucosa than the corresponding blank formulations. This is illustrated in Fig. 7. $SLN2_{TTAB\text{-}PNPP}$, $NLC1_{TTAB\text{-}PNPP}$ and $NLC2_{TTAB\text{-}PNPP}$ showed the highest increase in mucosal residence time that was 3.9, 4.4, 3.5-fold more prolonged than that of blank formulations. $SLN1_{TTAB\text{-}PNPP}$ showed a lower increase in mucosal residence time by 2.1-fold followed by 1.85 and 1.48-fold for $SEDDS1_{TTAB\text{-}PNPP}$ and $SEDDS2_{TTAB\text{-}PNPP}$, respectively. The increase in FDL remaining on the intestinal mucosa as shown in Fig. 7 correlated with the initial zeta potential difference between the blank formulation and the TTAB-PNPP modified nanocarriers (Figs. 1 and 4). In case of SEDDS, zeta potential of $SEDDS_{blank}$ was less negative than that of $SEDDS_{TTAB\text{-}PNPP}$ as shown in Figs. 1 and 4. $SLN2_{TTAB\text{-}PNPP}$, $NLC1_{TTAB\text{-}PNPP}$ and $NLC2_{TTAB\text{-}PNPP}$ initiated contact with mucus at a less negative zeta potential than the blank formulations, whereas $SLN1_{TTAB\text{-}PNPP}$ formulation started contact with mucus with the same zeta potential as $SLN1_{blank}$. It was also evaluated in previous study that the ability of phosphate modified nanocarriers with charge conversion to remain in the mucus was higher than without phosphate removal (Griesser et al., 2019).

Fig. 7 suggests three findings; (1) The lower ability of the nanocarriers to adhere to mucus in the presence of PIC2 indicates that IAP plays a role in charge conversion of lipid nanocarriers. (2) The concentration of IAP on intestinal mucosa is sufficiently high to cleave phosphate thereby altering the zeta potential of nanocarriers. (3) The initial zeta potential of modified lipid nanocarriers is an important factor influencing the ability of nanocarriers to interact with mucus upon contact with intestinal mucosa. In case of phosphate decorated lipid nanocarriers, the negative charges of nanocarriers did not cause repulsion by mucus resulting in the movement of nanocarriers into deeper mucus regions, followed by cleavage of phosphate groups by IAP leading to a shift in zeta potential from negative to positive. Furthermore, ionic bonds between the positively charged nanocarriers and the negatively charged mucus were formed resulting in the prolongation of mucosal residence time of these nanocarriers.

4. Conclusion

Lipid nanocarriers including SEDDS, SLN and NLC were decorated with the phosphorylated surfactant PNPP in order to prolong their mucosal residence time. The results of charge conversion studies due to IAP showed a shift from negative to positive charge for all formulations. Phosphate release studies using isolated IAP as well as Caco-2 cells showed a significantly higher phosphate release compared to control. Mucosal residence time studies demonstrated that modification of lipid nanocarriers provide a significant higher FDL concentration remaining on the intestinal mucosa compared to the blank formulations indicating that the contact time of phosphate decorated lipid nanocarriers was longer than that of the unmodified ones. Phosphate modified lipid nanocarriers might therefore be a promising tool to prolong mucosal residence times.

CRediT authorship contribution statement

Nuri Ari Efiana: Methodology, Investigation, Writing – original draft, Visualization, Writing – review & editing. **Andrea Fürst:** Investigation. **Ahmad Saleh:** Investigation. **Iram Shahzadi:** Investigation. **Andreas Bernkop-Schnürch:** Conceptualization, Writing – review & editing, Supervision, Project administration, Funding acquisition.

Declaration of Competing Interest

The authors declare that they have no known competing financial interests or personal relationships that could have appeared to influence the work reported in this paper.

Data availability

Data will be made available on request.

Acknowledgement

The authors would like to thank Ahmad Dahlan University for providing a travel grant.

References

Akkuş-Dağdeviren, Z.B., Nazir, I., Jalil, A., Tribus, M., Bernkop-Schnürch, A., 2019. Zeta Potential Changing Polyphosphate Nanoparticles: A Promising Approach To Overcome the Mucus and Epithelial Barrier. Mol. Pharm. 16 (6), 2817–2825. https://doi.org/10.1021/acs.molpharmaceut.9b00355.

Akkuş-Dağdeviren, Z.B., Wolf, J.D., Kurpiers, M., Shahzadi, I., Steinbring, C., Bernkop-Schnürch, A., 2021. Charge Reversal Self-Emulsifying Drug Delivery Systems: A Comparative Study among Various Phosphorylated Surfactants. J. Colloid Interface Sci. 589, 532–544. https://doi.org/10.1016/j.jcis.2021.01.025.

Almousallam, M., Moia, C., Zhu, H., 2015. Development of Nanostructured Lipid Carrier for Dacarbazine Delivery. Int. Nano Lett. 5 (4), 241–248. https://doi.org/10.1007/s40089-015-0161-8.

Baykov, A.A., Evtushenko, O.A., Avaeva, S.M., 1988. A Malachite Green Procedure for Orthophosphate Determination and Its Use in Alkaline Phosphatase-Based Enzyme Immunoassay. Anal. Biochem. 171 (2), 266–270. https://doi.org/10.1016/0003-2697(88)90484-8.

Carter, S.G., Karl, D.W., 1982. Inorganic Phosphate Assay with Malachite Green: An Improvement and Evaluation. J. Biochem. Biophys. Methods 7 (1), 7–13. https://doi.org/10.1016/0165-022x(82)90031-8.

Feeney, O.M., Williams, H.D., Pouton, C.W., Porter, C.J.H., 2014. 'Stealth' Lipid-Based Formulations: Poly(Ethylene Glycol)-Mediated Digestion Inhibition Improves Oral Bioavailability of a Model Poorly Water Soluble Drug. J. Controlled Release 192, 219–227. https://doi.org/10.1016/j.jconrel.2014.07.037.

Ghosh, S.S., Wang, J., Yannie, P.J., Cooper, R.C., Sandhu, Y.K., Kakiyama, G., Korzun, W. J., Ghosh, S., 2021. Over-Expression of Intestinal Alkaline Phosphatase Attenuates Atherosclerosis. Circ. Res. 128 (11), 1646–1659. https://doi.org/10.1161/CIRCRESAHA.120.317144.

Gradauer, K., Vonach, C., Leitinger, G., Kolb, D., Fröhlich, E., Roblegg, E., Bernkop-Schnürch, A., Prassl, R., 2012. Chemical Coupling of Thiolated Chitosan to Preformed Liposomes Improves Mucoadhesive Properties. Int. J. Nanomedicine 7, 2523–2534. https://doi.org/10.2147/IJN.S29980.

Griesser, J., Hetényi, G., Federer, C., Steinbring, C., Ellemunter, H., Niedermayr, K., Bernkop-Schnürch, A., 2019. Highly Mucus Permeating and Zeta Potential Changing Self-Emulsifying Drug Delivery Systems: A Potent Gene Delivery Model for Causal Treatment of Cystic Fibrosis. Int. J. Pharm. 557, 124–134. https://doi.org/10.1016/j.ijpharm.2018.12.048.

Griffin, B.T., Guo, J., Presas, E., Donovan, M.D., Alonso, M.J., O'Driscoll, C.M., 2016. Pharmacokinetic, Pharmacodynamic and Biodistribution Following Oral Administration of Nanocarriers Containing Peptide and Protein Drugs. Adv. Drug Deliv. Rev. 106, 367–380. https://doi.org/10.1016/j.addr.2016.06.006.

Grotz, E., Bernabeu, E., Pappalardo, M., Chiappetta, D.A., Moretton, M.A., 2017. Nanoscale Kolliphor® HS 15 Micelles to Minimize Rifampicin Self-Aggregation in Aqueous Media. J. Drug Deliv. Sci. Technol. 41, 1–6. https://doi.org/10.1016/j.jddst.2017.06.009.

Hens, B., Tsume, Y., Bermejo, M., Paixao, P., Koenigsknecht, M.J., Baker, J.R., Hasler, W. L., Lionberger, R., Fan, J., Dickens, J., Shedden, K., Wen, B., Wysocki, J., Loebenberg, R., Lee, A., Frances, A., Amidon, G., Yu, A., Benninghoff, G., Salehi, N., Talattof, A., Sun, D., Amidon, G.L., 2017. Low Buffer Capacity and Alternating Motility along the Human Gastrointestinal Tract: Implications for in Vivo Dissolution and Absorption of Ionizable Drugs. Mol. Pharm. 14 (12), 4281–4294. https://doi.org/10.1021/acs.molpharmaceut.7b00426.

Hirano, K., Matsumoto, H., Tanaka, T., Hayashi, Y., Lino, S., Domar, U., Stigbrand, T., 1987. Specific Assays for Human Alkaline Phosphatase Isozymes. Clin. Chim. Acta 166 (2), 265–273. https://doi.org/10.1016/0009-8981(87)90429-3.

Kali, G., Knoll, P., Bernkop-Schnürch, A., 2022. Emerging Technologies to Increase Gastrointestinal Transit Times of Drug Delivery Systems. J. Control. Release Off. J. Control. Release Soc. 346, 289–299. https://doi.org/10.1016/j.jconrel.2022.04.016.

Keck, C.M., Baisaeng, N., Durand, P., Prost, M., Meinke, M.C., Müller, R.H., 2014. Oil-Enriched, Ultra-Small Nanostructured Lipid Carriers (UsNLC): A Novel Delivery System Based on Flip-Flop Structure. Int. J. Pharm. 477 (1), 227–235. https://doi.org/10.1016/j.ijpharm.2014.10.029.

Kurpiers, M., Wolf, J.D., Steinbring, C., Zaichik, S., Bernkop-Schnürch, A., 2020. Zeta Potential Changing Nanoemulsions Based on Phosphate Moiety Cleavage of a PEGylated Surfactant. J. Mol. Liq. 316, 113868 https://doi.org/10.1016/j.molliq.2020.113868.

Le-Vinh, B., Steinbring, C., Wibel, R., Friedl, J.D., Bernkop-Schnürch, A., 2021. Size Shifting of Solid Lipid Nanoparticle System Triggered by Alkaline Phosphatase for Site Specific Mucosal Drug Delivery. Eur. J. Pharm. Biopharm. 163, 109–119. https://doi.org/10.1016/j.ejpb.2021.03.012.

Le-Vinh, B., Akkuş-Dağdeviren, Z.B., Le, N.-M.-N., Nazir, I., Bernkop-Schnürch, A., 2022. Alkaline Phosphatase: A Reliable Endogenous Partner for Drug Delivery and Diagnostics. Adv. Ther. 5 (2), 2100219. https://doi.org/10.1002/adtp.202100219.

Liu, L., Mao, K., Wang, W., Pan, H., Wang, F., Yang, M., Liu, H., 2016. Kolliphor® HS 15 Micelles for the Delivery of Coenzyme Q10: Preparation, Characterization, and Stability. AAPS PharmSciTech 17 (3), 757–766. https://doi.org/10.1208/s12249-015-0399-5.

López-García, J., Lehocký, M., Humpolíček, P., Sáha, P., 2014. HaCaT Keratinocytes Response on Antimicrobial Atelocollagen Substrates: Extent of Cytotoxicity, Cell Viability and Proliferation. J. Funct. Biomater. 5 (2), 43–57. https://doi.org/10.3390/jfb5020043.

Luan, J., Zhang, D., Hao, L., Qi, L., Liu, X., Guo, H., Li, C., Guo, Y., Li, T., Zhang, Q., Zhai, G., 2014. Preparation, Characterization and Pharmacokinetics of Amoitone B-Loaded Long Circulating Nanostructured Lipid Carriers. Colloids Surf. B Biointerfaces 114, 255–260. https://doi.org/10.1016/j.colsurfb.2013.10.018.

Mudie, D.M., Murray, K., Hoad, C.L., Pritchard, S.E., Garnett, M.C., Amidon, G.L., Gowland, P.A., Spiller, R.C., Amidon, G.E., Marciani, L., 2014. Quantification of Gastrointestinal Liquid Volumes and Distribution Following a 240 ML Dose of Water in the Fasted State. Mol. Pharm. 11 (9), 3039–3047. https://doi.org/10.1021/mp500210c.

Nazir, I., Fürst, A., Lupo, N., Hupfauf, A., Gust, R., Bernkop-Schnürch, A., 2019. Zeta Potential Changing Self-Emulsifying Drug Delivery Systems: A Promising Strategy to Sequentially Overcome Mucus and Epithelial Barrier. Eur. J. Pharm. Biopharm. Off. J. Arbeitsgemeinschaft Pharm. Verfahrenstechnik EV 144, 40–49. https://doi.org/10.1016/j.ejpb.2019.09.007.

O'Driscoll, C.M., Bernkop-Schnürch, A., Friedl, J.D., Préat, V., Jannin, V., 2019. Oral Delivery of Non-Viral Nucleic Acid-Based Therapeutics - Do We Have the Guts for This? Eur. J. Pharm. Sci. 133, 190–204. https://doi.org/10.1016/j.ejps.2019.03.027.

Perera, G., Zipser, M., Bonengel, S., Salvenmoser, W., Bernkop-Schnürch, A., 2015. Development of Phosphorylated Nanoparticles as Zeta Potential Inverting Systems. Eur. J. Pharm. Biopharm. 97, 250–256. https://doi.org/10.1016/j.ejpb.2015.01.017.

Rabanel, J.-M., Hildgen, P., Banquy, X., 2014. Assessment of PEG on Polymeric Particles Surface, a Key Step in Drug Carrier Translation. J. Control. Release Off. J. Control. Release Soc. 185, 71–87. https://doi.org/10.1016/j.jconrel.2014.04.017.

Schubert, M.A., Müller-Goymann, C.C., 2003. Solvent Injection as a New Approach for Manufacturing Lipid Nanoparticles – Evaluation of the Method and Process Parameters. Eur. J. Pharm. Biopharm. 55 (1), 125–131. https://doi.org/10.1016/S0939-6411(02)00130-3.

Severino, P., Andreani, T., Macedo, A.S., Fangueiro, J.F., Santana, M.H.A., Silva, A.M., Souto, E.B., 2012. Current State-of-Art and New Trends on Lipid Nanoparticles (SLN and NLC) for Oral Drug Delivery. J. Drug Deliv. 2012, 750891 https://doi.org/10.1155/2012/750891.

Sharifi, F., Nazir, I., Asim, M.H., Jahangiri, M., Ebrahimnejad, P., Matuszczak, B., Bernkop-Schnürch, A., 2019. Zeta Potential Changing Self-Emulsifying Drug Delivery Systems Utilizing a Novel Janus-Headed Surfactant: A Promising Strategy for Enhanced Mucus Permeation. J. Mol. Liq. 291, 111285 https://doi.org/10.1016/j.molliq.2019.111285.

Sis, H., Birinci, M., 2009. Effect of Nonionic and Ionic Surfactants on Zeta Potential and Dispersion Properties of Carbon Black Powders. Colloids Surf. Physicochem. Eng. Asp. 341 (1), 60–67. https://doi.org/10.1016/j.colsurfa.2009.03.039.

Suchaoin, W., Pereira de Sousa, I., Netsomboon, K., Lam, H.T., Laffleur, F., Bernkop-Schnürch, A., 2016. Development and in Vitro Evaluation of Zeta Potential Changing Self-Emulsifying Drug Delivery Systems for Enhanced Mucus Permeation. Int. J. Pharm. 510 (1), 255–262. https://doi.org/10.1016/j.ijpharm.2016.06.045.

Wissing, S.A., Kayser, O., Müller, R.H., 2004. Solid Lipid Nanoparticles for Parenteral Drug Delivery. Adv. Drug Deliv. Rev. 56 (9), 1257–1272. https://doi.org/10.1016/j.addr.2003.12.002.

Wolf, J.D., Kurpiers, M., Götz, R.X., Zaichik, S., Hupfauf, A., Baecker, D., Gust, R., Bernkop-Schnürch, A., 2020. Phosphorylated PEG-Emulsifier: Powerful Tool for Development of Zeta Potential Changing Self-Emulsifying Drug Delivery Systems (SEDDS). Eur. J. Pharm. Biopharm. 150, 77–86. https://doi.org/10.1016/j.ejpb.2020.03.004.